DESIGN OF POLAR-SEPARABLE FIR FILTERS BY RADIAL SLICE APPROXIMATIONS

Richard Rau and James H. McClellan

School of Electrical and Computer Engineering
Georgia Institute of Technology
Atlanta, GA 30332-0250

ABSTRACT

We introduce the design of polar-separable 2-D FIR filters by radial slice approximations (RSA). It is a two step procedure. First, 1-D filters for the radial and the angular components are designed. Then the desired filter response is approximated on many radial slices in a weighted mean square sense. In the case of circular filters, RSA outperforms other design procedures in terms of ripple size and circularity of the passband. Examples of filters with non-constant angular functions prove the flexibility of the new method.

1. INTRODUCTION

The design of 2-D FIR filters for signal and image processing is an important and difficult problem. Several image processing techniques [1, 2] require FIR filters that are polar-separable in the ideal case. We present here a general two step procedure called Radial Slice Approximations (RSA) to design FIR filters with arbitrary angular and radial specifications in the frequency domain. First 1-D filters for the radial and angular components are designed. Then the impulse response is obtained by approximating the radial filters weighted by the angular components along radial slices. The resulting filter design equations have the form of an unconstrained deconvolution problem and can be solved efficiently.

2. POLAR-SEPARABLE FILTERS

A continuous 2-D function $D(x,y)$ is polar-separable, if it can be written as a product of a purely angular and a purely radial component in polar coordinates. Since the frequency response of 2-D discrete filters is 2π-periodic in each direction, polar-separable discrete filters in the strict sense do not exist. Instead, we consider here filters of the ideal form (see Fig. 1):

$$D(\omega_1,\omega_2) = \begin{cases} R(\omega)A(\phi) & \text{if } \omega \le \pi \\ 0 & \text{in rest of freq. cell} \end{cases} \qquad (1)$$

with $\omega = \sqrt{\omega_1^2+\omega_2^2}$, $\omega \in [0,\pi]$ and $\phi = \arg(\omega_1,\omega_2)$, $\phi \in [0,2\pi)$. To avoid ambiguities special care has to be taken for $\omega = 0$. Two cases are possible:

1. $R(0) \neq 0$ requires that $A(\phi) = \text{const.} \forall \phi \in [0,2\pi)$.
2. $R(0) = 0$ permits $A(\phi)$ to be arbitrary.

Thus, lowpass filters can only be circular symmetric. We restrict ourselves to real coefficient filters. In this case $R(\omega)$ can be chosen real without loss of generality and the angular component becomes $A(\phi) = A_e(\phi) + jA_o(\phi)$ with $A_e(\phi)$ being real and even-harmonic and $A_o(\phi)$ being real and odd-harmonic.

The proposed filter design technique exploits the fact that radial slices of $D(\omega_1,\omega_2)$ on the π-disk, as shown in Fig. 1, can be viewed as the frequency responses of 1-D filters.

If we extend $R(\omega)$ into an even function

$$R_e(\omega) = R(\omega)\chi_{[0,\pi]}(\omega) + R(-\omega)\chi_{[-\pi,0)}(\omega) \qquad (2)$$

and an odd function

$$R_o(\omega) = R(\omega)\chi_{[0,\pi]}(\omega) - R(-\omega)\chi_{[-\pi,0)}(\omega) \qquad (3)$$

with the indicator function $\chi_{[a,b]}$ defined on the interval $[a,b]$, a radial slice $S_\beta^D(\omega) = D(\omega\cos\beta, \omega\sin\beta)$, $\omega \in [-\pi,\pi]$ for any $\beta \in [0,2\pi)$ can be written as

$$S_\beta^D(\omega) = R_e(\omega)A_e(\beta) + jR_o(\omega)A_o(\beta) \qquad (4)$$

The inverse DTFT of (4) with respect to ω is

$$s_\beta^D(n) = r_e(n)A_e(\beta) + r_o(n)A_o(\beta) \qquad (5)$$

where $r_e(n)$ and $r_o(n)$ are even and odd real valued sequences, respectively.

3. APPROXIMATION OF RADIAL SLICES

Filters of the form (1) are IIR and are, therefore, not practical in most cases. Instead, we present a procedure to design 2-D FIR filters which approximate the ideal filters closely.

Let $f(n_1,n_2)$ denote the 2-D impulse response of the FIR filter to be designed with a region of support (ROS) of size $N \times N$. In the design, the ROS of $f(n_1,n_2)$ needs to be centered at the origin of the coordinate system. Hence, if N is even, we work on the grid of mid-integer points $(\mathbf{Z}+\frac{1}{2}) \times (\mathbf{Z}+\frac{1}{2})$.

There is a linear β-dependent operator which maps $f(n_1,n_2)$ into its radial slice $s_\beta^F(n)$ defined on the π-disk:

$$s_\beta^F(n) = \sum_{k,l \in \text{ROS}} f(k,l)\,\text{Sl}_\beta(n,k,l) \qquad (6)$$

This work was supported by the Joint Services Electronics Program under contract DAAH-04-96-1-0161

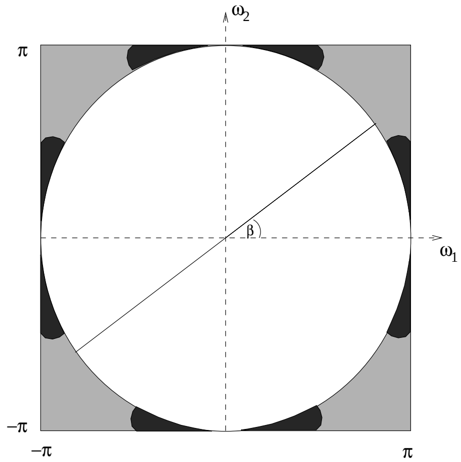

Figure 1: General specifications of polar-separable FIR filters.

with the kernel

$$\mathrm{Sl}_\beta(n,k,l) = \mathrm{sinc}(\pi(n - k\cos\beta - l\sin\beta)) \tag{7}$$

and with $n,k,l \in \mathbf{Z}$ or $(\mathbf{Z}+\frac{1}{2})$, respectively. Although $f(n_1,n_2)$ has finite support, $s_\beta^F(n)$ can have infinite support. Equation (6) can be viewed as a discrete, bandlimited version of the Projection-Slice Theorem.

The filter $F(\omega_1,\omega_2)$ approximates $D(\omega_1,\omega_2)$ on the π-disk well, if $s_\beta^F(n) \approx s_\beta^D(n)$, $\forall\beta$. This criterion is used to design $F(\omega_1,\omega_2)$ by approximating $s_\beta^D(n)$ for several β simultaneously. We minimize for each slice the mean squared error $\| s_\beta^D(n) - s_\beta^F(n) \|_2^2$. The resulting normal equations for the approximation of one slice are:

$$\sum_{p,q\in\mathrm{ROS}} \mathrm{K}_\beta(k-p,l-q)f(p,q) = \sum_n s_\beta^D(n)\mathrm{Sl}_\beta(n,k,l) \tag{8}$$

with $k,l \in \mathrm{ROS}$. The kernel

$$\mathrm{K}_\beta(k-p,l-q) = \sum_{m=-\infty}^{\infty} \mathrm{Sl}_\beta(m,k,l)\mathrm{Sl}_\beta(m,p,q) \tag{9}$$

can be evaluated in closed form by rewriting the sum as a convolution of ideal brickwall lowpass filters with fractional delays. It is

$$\mathrm{K}_\beta(k,l) = \mathrm{sinc}(\pi(k\cos\beta + l\sin\beta)) \tag{10}$$

The left side of (8) is a 2-D convolution. Approximating many slices simultaneously leads to a multi-objective optimization problem of the form

$$\min_f \max_{\beta_\nu} \| s_{\beta_\nu}^D(n) - s_{\beta_\nu}^F(n) \|_2^2 \tag{11}$$

which is difficult to solve. Instead we use a weighted least squares approach. In this paper our results were obtained with a uniform weight distribution. A recursive weighted least squares method to solve (11) approximately is currently under investigation.

Since the approximation of radial slices specifies the frequency response only inside the π-disk, we need additional constraints to force the gray and black areas of Fig. 1 to zero. The minimization of the signal energy in those frequency regions in the mean square sense can easily be incorporated into our framework. The corresponding normal equations are homogeneous and contain a kernel of the form:

$$\mathrm{E}_1(k,l) = \delta(l)\delta(k) - \frac{J_1(\pi\sqrt{l^2+k^2})}{2\sqrt{l^2+k^2}} \tag{12}$$

where $J_1(\cdot)$ is the Bessel function of the first kind of order 1. If the frequency responses of $r_e(n)$ and of $r_o(n)$ are not zero at $\omega = \pi$, this additional error constraint does not suppress the signal energy in the black areas of Fig. 1 sufficiently, which can lead to high ripples. Several additional constraints are possible. The most effective solution was found to be minimizing the energy along the edges of the frequency cell. The error kernel is:

$$\mathrm{E}_2(k,l) = (-1)^k\delta(l) + (-1)^l\delta(k) \tag{13}$$

The set of filter design equations is a linear combination of the normal equations for several slices and for the two energy constraints:

$$(w_{\mathrm{E}_1}\mathrm{E}_1 + w_{\mathrm{E}_2}\mathrm{E}_2 + \sum_{\beta_k\in B} w_{\beta_k}\mathrm{K}_{\beta_k}) ** f = \sum_{\beta_k\in B} w_{\beta_k}\langle s_{\beta_k}^D, \mathrm{Sl}_{\beta_k}\rangle_n \tag{14}$$

where $**$ denotes 2-D convolution and $\langle\cdot,\cdot\rangle_n$ the summation with respect to n. B denotes the set of slice angles. The relative importance of the different error terms can be adjusted with the weights w_ν.

4. DESIGNING THE RADIAL AND ANGULAR COMPONENTS

Mean square error filters can locally deviate significantly from the desired frequency response. Therefore, other error criteria like Chebyshev approximation are often employed. However, they lead to computationally very expensive algorithms, especially in the 2-D case.

Since RSA is based on minimizing a mean square error criterion, it is subject to the same kind of local deviations. In order to reduce them while keeping the simple set of design equations (14), we suggest a two step design procedure:

1. Modify $R(\omega)$ and $A(\phi)$ such that they can be approximated well in the mean square sense.
2. Compute $f(n_1,n_2)$ by solving (14).

The modification of $R(\omega)$ is based on the following observation. In the special case $\beta = 0$ (6) simplifies to

$$s_0^F(n) = \sum_l f(n,l) \tag{15}$$

A similar relationship holds for $\beta = \frac{\pi}{2}$. Thus, the best achievable approximation of the frequency slice responses for $\beta = 0$ and for $\beta = \frac{\pi}{2}$ is equal to the one obtainable by a 1-D FIR filter of length N. It is a lower bound on the overall achievable approximation error. In order to approach this error bound we approximate $R_e(\omega)$ and $R_o(\omega)$ with N tap filters $r_e^{ap}(n)$ and $r_o^{ap}(n)$ optimally in some sense and use them instead of $r_e(n)$ and $r_o(n)$ in (5).

The angular component $A(\phi)$ is approximated by a finite Fourier series. We obtained filters with very good properties, if the Fourier series contained approximately the first $\frac{N}{2}$ terms. If the series is much longer, considerable deviations from the desired filter occur especially in the stopbands.

5. DISCUSSION OF THE DESIGN EQUATIONS

The two-step design of polar-separable FIR filters uses the unconstrained deconvolution problem (14) to transform the 1-D radial and angular filters into a 2-D non-separable impulse response. In this respect RSA belongs to the family of filter design transformation techniques like the McClellan transformation.

The expressions in (14) can be determined easily. The left side of (14) depends only on N, B, and on the weights w_ν, but not on radial or angular filter specifications. This is an advantage, if several filters of the same size but with different passband properties have to be designed. The symmetries

$$\mathrm{E}_1(k,l) = \mathrm{E}_1(-k,l) = \mathrm{E}_1(k,-l) = \mathrm{E}_1(-k,-l)$$
$$\mathrm{E}_2(k,l) = \mathrm{E}_2(-k,l) = \mathrm{E}_2(k,-l) = \mathrm{E}_2(-k,-l)$$
$$\mathrm{Sl}_\beta(n,k,l) = \mathrm{Sl}_\beta(-n,-k,-l)$$
$$\mathrm{K}_\beta(k,l) = \mathrm{K}_\beta(-k,-l)$$

reduce the amount of computation for each term in (14) by a factor of four or two, respectively. Furthermore, if the β_ν are symmetric with respect to $\frac{\pi}{2}$ and $\frac{\pi}{4}$, the symmetries

$$\mathrm{K}_\beta(k,l) = \mathrm{K}_{\frac{\pi}{2}-\beta}(l,k) = \mathrm{K}_{\frac{\pi}{2}+\beta}(-l,k) = \mathrm{K}_{\pi-\beta}(-k,l)$$

$$\mathrm{Sl}_\beta(\cdot,k,l) = \mathrm{Sl}_{\frac{\pi}{2}-\beta}(\cdot,l,k) = \mathrm{Sl}_{\frac{\pi}{2}+\beta}(\cdot,-l,k) = \mathrm{Sl}_{\pi-\beta}(\cdot,-k,l)$$

decrease the number of evaluations of $\mathrm{sinc}(\cdot)$ by another factor of four.

Written as matrices E_1, E_2 and K_{β_k} in (14) are symmetric Toeplitz-Block-Toeplitz. In general, these matrices are not full rank. However, there is experimental evidence that (14) can always be made full rank by using a "sufficient" number of slices with different β_k. In general, the larger N is, the more slices are necessary. A symmetric $N^2 \times N^2$ Toeplitz-Block-Toeplitz matrix is completely specified by $2N^2 - 2N + 1$ values. Fast algorithms exist to solve this general class of linear equation systems with $O(N^3 \log_2^2 N)$ floating point operations [4]. In MATLAB the built in equation solver is sufficiently fast for filters with $N \approx 30$.

In its general form (14) has many degrees of design freedom. For most filters of interest, equally angular spaced β_ν are a natural choice. A large number of slices supports good circular properties of the designed filter, but can cause high stopband and passband ripples for small N. In most cases we used uniform weight distributions for w_k. Some experiments suggest that non-uniform weight distributions can improve the circularity of the designed filters for small N. The weights w_{E_1} and w_{E_2} can often be varied considerably, without changing the filter properties significantly.

Method	δ_p	δ_s
RSA	0.0308	0.0289
NDFT	0.0324	0.0519
Uniform Sampling	0.0393	0.0519
Nonuniform LLS	0.0360	0.0430
McClellan Transformation	0.0238	0.0238
Hazra-Reddy Transformation	0.0587	0.0587

Table 1: Passband and stopband ripples for circular lowpass filter designed with different techniques. (Parts of the table have been taken from [3].)

6. DESIGN EXAMPLES

First we consider circular symmetric lowpass filters - a common class of polar-separable filters. If $s_\beta^D(n)$ is a 1-D equiripple filter, circular 2-D filter designed with RSA are nearly equiripple in most cases. We designed a 15×15 filter with passband edge $\omega_p = 0.4\pi$ and stopband edge $\omega_s = 0.6\pi$. We used 48 equally spaced and uniformly weighted radial slices and set $w_{E_1} = 1$ and $w_{E_2} = 1$. The ripples of the obtained filter were compared to data given in [3] for filters designed with nonuniform frequency sampling (NDFT), uniform frequency sampling, nonuniform frequency sampling using a linear least square (LLS) approach, the McClellan transformation and the frequency transformation proposed by Hazra and Reddy. Please see [3] for references. Table 1 shows that only the McClellan transformation outperforms RSA. However, RSA produces filters with better passband circularity than the McClellan transformation. This becomes more significant for increasing ω_p. Figure 2 shows the case for $\omega_p = 0.7\pi$ and $\omega_s = 0.9\pi$. Another advantage over the McClellan transformation is that even length filters can be designed. In fact in most cases these new filters are of exceptional quality with high circularity and ripple sizes very close to the ripples of the 1-D prototype. Figure 3 shows the frequency response of a 12×12 filter with $\omega_p = 0.4\pi$ and $\omega_s = 0.6\pi$. We used 48 equally spaced and uniformly weighted radial slices and set $w_{E_1} = 0.5$, $w_{E_2} = 0$. The ripples are $\delta_p = 0.0553$ and $\delta_s = 0.0568$ compared to $\delta = 0.0552$ of the 1-D equiripple filter.

To demonstrate the full flexibility of RSA, we designed a 22×22 wedge shaped bandpass filter with a real frequency response as it is used in image decomposition techniques based on properties of the human visual system [1]. We used an equiripple bandpass filter with $\omega_{s_1} = 0.15\pi$, $\omega_{p_1} = 0.3\pi$, $\omega_{p_2} = 0.7\pi$ and $\omega_{s_2} = 0.85\pi$ for $r_e^{ap}(n)$. $A_e(\phi)$ was obtained by first designing a zero phase equiripple lowpass filter of length $N = 21$ with $\omega_p = 0.1\pi$ and $\omega_s = 0.3\pi$ and then by setting the impulse response values to zero for all odd n to make it even harmonic. The designed filter shown in Fig. 4a,b approximates the product of the two 1-D filters closely. The plot of concentric circular slices of the filter frequency response for radii $\omega = 0.25\pi$, $\omega = 0.5\pi$ and $\omega = 0.75\pi$ in Fig. 5 shows that deviations from the angular prototype filter are small and occur mostly in the stopbands. Therefore, RSA is particularly useful to design FIR filters, which require very accurate angular components such as steerable filters [2].

7. REFERENCES

[1] T. G. Campbell et al., "Image Sequence Representation using Polar Separable Filters", Proceedings of the SPIE, vol. 1360, pt.2, pp.1126-33, 1990

[2] W. T. Freeman et al., "The Design and Use of Steerable Filters", IEEE Trans. on Pattern Analysis and Machine Intelligence, vol. 13, no. 9, pp.891-906, 1991

[3] S. Bagchi, "The Nonuniform Discrete Fourier Transform and its Applications in Signal Processing", PhD Thesis, University of California Santa Barbara, Dec. 1994

[4] Y. Wang et al., "On Fast and Superfast Algorithms for Solving Block Toeplitz Systems", Twenty-Third Asilomar Conference on Signals, Systems and Computers, vol. 2, pp.643-7, 1989

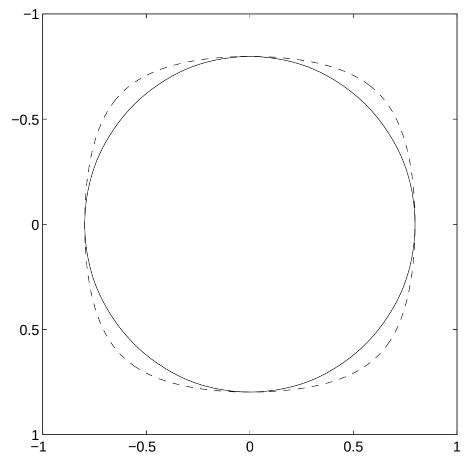

Figure 2: Contour plot at amplitude 0.5 for a lowpass filter with $\omega_p = 0.7\pi$ and $\omega_s = 0.9\pi$ designed with RSA (solid line) and with the McClellan transformation (dashed line).

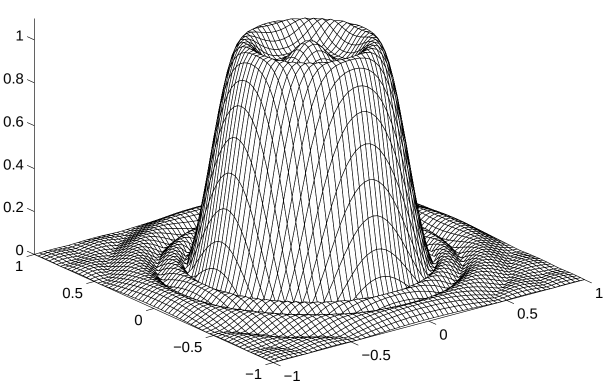

Figure 3: 12×12 lowpass filter with $\omega_p = 0.4\pi$ and $\omega_s = 0.6\pi$

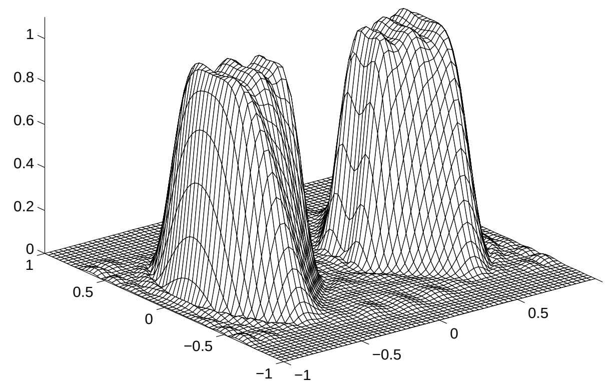

(a) Frequency response

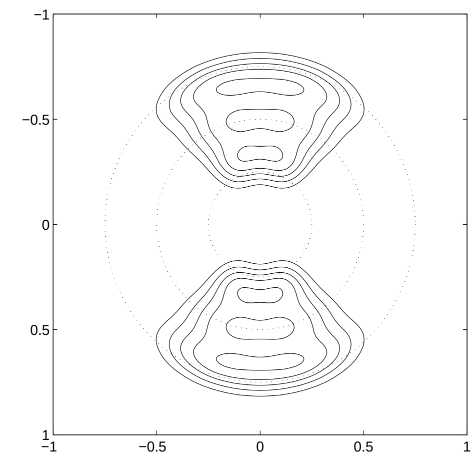

(b) Contour plot

Figure 4: 22×22 wedge shaped bandpass filter. (a) Frequency response. (b) Contour plot.

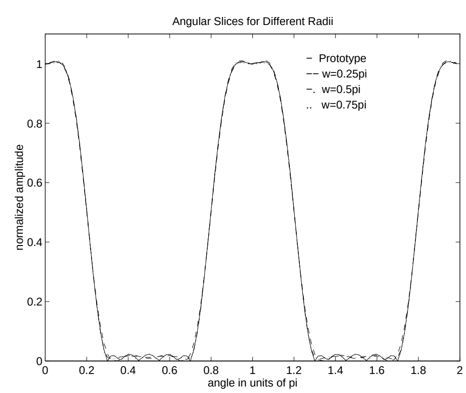

Figure 5: Concentric circular slices through the frequency response of the wedge shaped bandpass filter, as marked in Fig. 4b